Cell Model and Computer Simulation Studies of Layered and Hexagonal States of Aligned, Hard Disks versus Rods

M. F. Sharlow,[†] R. L. B. Selinger,[‡,⊥] A. Ben-Shaul,[§] and W. M. Gelbart*,[†]

Department of Chemistry and Biochemistry, University of California, Los Angeles, Los Angeles, California 90024; Institute for Physical Science and Technology, University of Maryland, College Park, Maryland 20742; and Department of Physical Chemistry and The Fritz Haber Center, The Hebrew University, Jerusalem, Israel 91904

Received: August 30, 1994; In Final Form: November 12, 1994[⊗]

We consider the possibility of smectic and columnar phases in fluids and colloidal suspensions of aligned rods and disks interacting through excluded-volume forces. After briefly reviewing previous work, and applying known cell model techniques to compare the phase behaviors of disks and rods, we present and discuss the results from new Monte Carlo simulations of perfectly oriented rods (spherocylinders) and disks (torocylinders). We conclude tentatively that columnar phases are stable only in the case of disks.

I. Introduction

As much as 40 years ago, Onsager[1] developed a density-expansion theory which accounted for the spontaneous onset of long-range orientational order when an isotropic suspension of sufficiently anisotropic hard rods is concentrated. This theory, extended systematically to incorporate higher-order virial corrections[2] and attractive forces,[3] survives to the present day as the qualitatively correct approach to the essential physics of the isotropic (I) to nematic (N) transition. Nevertheless, and not for want of trying,[4] more than 30 years went by before a clear I-to-N phase change was observed definitively via computer simulation.[5] Experimentally, this phenomenon had been reported for dilute suspensions of long and thin rods of tobacco mosaic virus (TMV)[1,6] (see also ref 7). As predicted by the Onsager theory, the spontaneous alignment appears at a volume fraction which varies with width-to-length ratio according to $\phi^* \simeq D/L$. For $\phi > \phi^*$ the packing entropy terms, involving the number of ways to pack ("fit in") the hard particles, dominate over the orientational disorder contributions, and the overall free energy is minimized by the singling out of a preferred direction for the rod axes. This situation is in many ways analogous to the freezing transition in hard-sphere systems where, at high enough ϕ, the overall entropy is actually increased, and the free energy decreased, upon the onset of long-range order. Such systems can pack more efficiently (i.e., in more ways) when ordered; hence, they tend to give up their positional disorder.[8]

One of the most exciting recent developments in colloidal/liquid crystal science has been the discovery, via computer simulation, of a sequence of partially positionally ordered phases in fluids composed of hard rods.[9] Here the initial surprise was that the aligned rods, at first in a nematic phase, would choose to go into stacked layers (smectic, or S, phase) or hexagonally ordered columns (columnar, or C, phase) without the benefit of any attractive interactions. (Experimentally, the smectic phases of colloidal suspensions of rigid rods also have been observed.[10]) In fact, these successive partial positional orderings can be understood in terms of the same kind of hard particle packing arguments that account for the I- to -N transition and for hard-sphere freezing. Accordingly, quasi-analytical theories for the packing of hard rods have been developed by many different groups,[11−15] with the specific aim of accounting for the "extra" smectic and/or columnar phases found in the simulation studies. These theories can be regarded as approximate treatments of the packing entropies as a function of successive positional orderings in one (smectic), two (columnar), and three (crystal) dimensions; they are sufficient to explain the sequence of transitions observed upon increase in density and the progressive disappearance of these intermediate phases upon increase in D/L. (In the hard-sphere limit, of course, only the crystal (or X) phase survives, whereas for intermediate axial ratios one has N → S → X, N → S → C → X, etc.)

Several more recent theoretical efforts have extended further our understanding of the smectic and columnar phases of colloidal suspensions. First, there are treatments of polydisperse systems of rods, of special interest because of the broad size distribution typical of most micellized surfactant solutions. Taylor and Herzfeld,[16] for example, have shown in particular how—with increasing temperature—the nematic phase gets "squeezed out" of existence between isotropic and positionally ordered (columnar or smectic) states in self-assembling lyotropic systems of polydisperse rods or disks. And Stroobants has destabilized the smectic phase in favor of the columnar by mixing long rods into short ones.[17] This last finding is consistent with the formation of hexagonal (vs smectic) phases in solutions of micellar rods, which have large intrinsic polydispersity.[16,18] (Conversely, one expects polydisperse micellar *disks* to form *smectic* rather than columnar states, as recently discussed by Boden and co-workers;[19] see also refs 16 and 18 for inclusion of polydispersity effects.) Also, while virtually all of the simulation studies and density-functional theories mentioned above start from the simplifying premise that orientational order in the nematic is perfectly saturated before transitions to smectic or columnar states occur, other studies have explored the effects of a distribution of orientations.[13,20,21a] Finally, attention has been addressed to the case of *oblate* hard particles, i.e., disks, and the effect of this new symmetry on the existence and sequence of N → S, C, X phase changes; see refs 16, 22, and 23. It is this latter point that we pursue further in the present communication.

* To whom correspondence should be addressed.
† University of California, Los Angeles (contact M.F.S. c/o W.M.G.).
‡ University of Maryland.
§ The Hebrew University.
⊥ Current address: Materials Science and Engineering Laboratory, National Institute of Standards and Technology, Gaithersburg, Maryland 20899.
⊗ Abstract published in *Advance ACS Abstracts,* February 1, 1995.

0022-3654/95/2099-2907$09.00/0

In the following section we outline briefly some results of approximate, quasi-analytical theories of partial positional ordering in aligned fluids of hard rods and disks. This allows us to introduce definitions and terminology relevant to the phase behavior of these systems and to provide a context (and results for comparison) for our Monte Carlo simulations. We base this discussion on a simple decomposition—due to Taylor, Hentschke, and Herzfeld[11]—of the free energy of perfectly oriented hard particles into separate contributions from the entropies of mixing, positional disorder, and packing. Because of the saturated alignment and the "confinement" into layers and columns, calculation of the "packing" terms for the smectic and columnar phases is shown to follow from consideration of hard particle statistical mechanics in two and one dimensions, respectively. The essential work on the comparison of rods and disks via this model was done by Taylor, who determined phase diagrams for rods and disks in his doctoral dissertation.[24] In these calculations (and in our cell model results, which are closely related), the columnar phase is found to be stable for both disks and rods, in contrast with the data obtained in our present Monte Carlo simulations.

The results of our constant pressure simulations are presented in section III. We treat in detail the case of spherocylindrical rods and torocylindrical disks, each with axial ratio 5:1. Comparisons are made between "small" and "large" system sizes to check the importance of unphysical diffusion effects in the stabilization of phases (see below). Initial states involving either highly ordered or disordered configurations (each with alternately large and small volumes) are chosen to test the equilibrium nature of "final" states. In analyzing the structure of these final configurations, we examine a variety of pair distribution functions involving "parallel" (with respect to alignment) and "normal" correlations between particles within the same, and different, layers or columns. At a pressure intermediate between solid and smectic states, we find that the disks form a stable columnar phase whereas the rods do not, in contrast to the cell model predictions of section II. Concluding discussion is offered in section IV, where we also mention the role of residual orientational disorder and alternate particle shapes in determining the relative stabilities of the smectic and columnar phases.

II. Cell Model Predictions

We begin with a key simplification motivated by the fact that orientational order is nearly saturated in all the liquid crystalline phases involved in our present study. In the original Onsager theory[1] of the I → N transition, the nematic phase first appears with a "P_2" order parameter as large as ≈0.9; upon concentration of the nematic, this order parameter increases further. Experimental determinations of $\langle P_2 \rangle$ indicate[7] comparably large values; even in the nematic state, then, the alignment of long rods appears to be almost complete—in the more concentrated smectic, columnar, and crystal phases it is still further saturated. Consistent with these facts, the computer simulation[9] and many of the quasi-analytical theories cited above are based on the simplifying assumption of perfect orientational order. In extending theoretical considerations to the case of oblate colloidal particles, we shall also feature this condition of compete alignment: by so doing we are able to expose most clearly the fundamental physics underlying the relative stabilities of layered and hexagonal phases of rods and disks.

To illustrate the basic idea, consider first the case of rods in smectic phases. Figure 1a shows schematically a small region in the cross section of a typical nematic configuration. Note

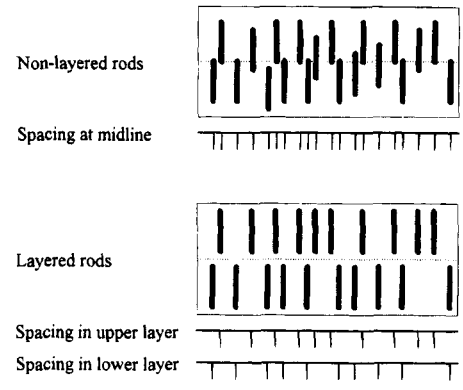

Figure 1. (a) Schematic picture of nematic ordering for rods of length L. The line below with tick marks illustrates the distribution of nearest-neighbor separations. (b) Schematic picture of smectic ordering in layers. The larger nearest-neighbor separations (see tick marks) illustrate the relief of packing congestion.

that the lateral packing entropy is relatively low because each rod can only move to the side a small distance before getting in the way of a neighbor (see line with ticks depicting lateral nearest-neighbor spacings). In Figure 1b, where the rods have been segregated into layers, this average spacing has been significantly increased, and the lateral packing entropy is concomitantly higher. Conversely, of course, the layering implicit in the smectic situation (1b) involves a loss of positional disorder. But at sufficiently high concentration, the packing entropy gain in the layers will dominate, and smectic order will appear spontaneously. This competition between loss of long-range disorder in the perpendicular dimension, in favor of more efficient lateral packing, is analogous to that between entropy terms in the I → N and freezing transitions mentioned above in the Introduction.[14]

Because of the segregation of rods into layers, one can compute the smectic free energy per particle by considering only a single layer. (In effect, this is done in ref 11.) Furthermore, the corrections to ideal fluid behavior can be separated into a *positional* entropy term involving long-range ordering (of the layers) in $d = 1$ dimension and a contribution describing the *interactions* of the particles (within the layers) in $3 - d = 2$ dimensions (see ref 11). Indeed, the interaction contributions to the free energy depend only upon the two-dimensional packing fraction. Similarly, in the case of a columnar phase, the rods interact within a single column and the relevant dimensionless concentration for the columns is the (1D) length fraction, corresponding to the fact that positional ordering here (hexagonal) involves $d = 2$ dimensions, so that the particles only interact with each other in $3 - d = 1$ dimensions. For the crystalline phase, in the spirit of the free energy decompositions introduced for the smectic and columnar phases—which involved positional ordering in one ($d = 1$) and two (d = 2) dimensions, respectively, with corresponding ($3 - d$)-dimensional fluid disorder—Taylor et al. have let $d = 3$ and effectively confined each particle to a "zero-dimensional" cell (that is, a small—molecular scale—polyhedron surrounding the particle). Accordingly, there are no fluid interaction ("packing") contributions, and the free energy consists only of "ideal" and "positional entropy loss" parts and involves ϱ_{cp}, the close-packed value of the number density of the hard, aligned, particles. Finally, for the nematic phase, "$d = 0$", i.e., there is no long-range positional ordering. Hence, no positional contribution arises, and packing must include excluded-volume effects in $3 - d = 3$ dimensions, involving the full (3-D) volume fraction ϕ. Note that the lower-dimensional concentration (2-D or 1-D)

is linearly proportional to ϕ via the first (second) power of the ratio of the layer (column) spacing to the rod length (diameter).

All of the packing free energy contributions defined above can be evaluated analytically, via either the scaled particle theory (SPT) (see refs 25 and 26) or y-expansion[27] approximations, as explicit functions of the 3-D packing fraction ϕ for the nematic (N) and solid (X) phases, of ϕ and the layer spacing λ for the smectic (S), and of ϕ and the column spacing λ' for the columnar (C). Minimizing the columnar (f_C) and smectic (f_S) free energies with respect to λ' and λ, respectively, leads to f_C and f_S as functions of ϕ only. These can be analyzed straightforwardly together with f_C and f_S, e.g., via common tangent constructions.

While the above discussion has been couched in terms of rod-shaped particles, it applies equally well to disks. The actual shape which we choose for the hard particles is that of the *sphero/torocylinder* of diameter D and length L. The prolate ("rod") form of this shape is the spherocylinder, consisting of a cylinder (of length L) "capped" at each end by a half-sphere (diameter D), while its oblate ("disk") form is the *torocylinder* (previously called the oblate spherocylinder), consisting of the same right circular cylinder but with a half-torus "wrapped" around its side. Note that the total length of the spherocylinder is $L + D$, corresponding to *total* axial ratio $(L + D)/D$, whereas the total diameter of the torocylinder is $D + L$, with axial ratio $(D + L)/L$. As $L \to 0$ in the former case and $D \to 0$ in the latter, the "rod" or "disk" particle shape reduces to a sphere. Thus, we can consider naturally the continuous evolution of anisotropy from prolate through oblate, with the familiar hard sphere comprising a convenient "zero"—or "mid"—point of reference.

The free energies discussed above apply directly to sphero- and torocylindrical particles as long as one is careful to take $L + D$ (instead of L) for the length ("height") of the rods in the smectic phase and $L + D$ (instead of D) for the diameter of the disks in the columnar phase. (Note that we neglect the complications due to less than perfect collinearity of spherocylinders in the column and to less than perfect coplanarity of torocylinders in the smectic state.) To evaluate the free energy of packing for the nematic, using the y expansion, we need to determine the dimensionless 3-D virial coefficients B_2 and B_3 for aligned sphero- and torocylinders. $B_2 = 4$ for *all* (prolate and oblate) convex hard particles in 3-D. But B_3 depends on particle shape and (so far as we are aware) is not known analytically for spherocylinders, even when they are aligned; we approximate it by its value for aligned (prolate or oblate) ellipsoids, which is the same as that for spheres (see ref 2), namely, $B_3 = 10$. Finally, to deal with the crystalline free energies, we use[25] $\varrho_{cpr} = 2/\{\sqrt{3}D^3[(L/D) + \sqrt{(2/3)}]\}$ for spherocylinders ("r" in the subscript denoting "rod"), reducing in the limit $L \to 0$ to the well-known hard-sphere (diameter D) value of $\sqrt{2}/D^3$. Thus, ϱ_{cp} corresponds—for all axial ratios—to the rods packing hexagonally, with their half-spherical caps "nestling" into each other as if they were the halves of close-packed spheres. Note that, in the long-rod limit ($L \to \infty$), $\nu\varrho_{cpr}$ tends (with particle volume $\nu \to \pi D^2 L/4$) to $\pi/\sqrt{12}$, the close-packing volume fraction for 2D disks.

For torocylinders, on the other hand, we find that the form of ϱ_{cp} depends on whether the axial ratio is large or small. For disks which are almost spheres (i.e., $(D + L)/L \approx 1$), close packing corresponds to a minor perturbation of that for spheres: each layer of aligned disks "nestles down" into the "holes" between those in the layer below. For this case, we have arrived at the expression ("d" for "disk") $\varrho_{cpd1} = 2/\{\sqrt{3}(L + D)^2(L^2 - {}^1/_3[L + (1 - \sqrt{3})D]^2)^{1/2}\}$, which reduces as it must to $\sqrt{2}/L^3$ in the $D \to 0$ (i.e., spheres of diameter L) limit. (A derivation of this expression is given in the Appendix.) For large torocylinders, on the other hand, close packing corresponds to successive layers of aligned disks lying a distance L apart, i.e., no "nestling." Here we find $\varrho_{cpd2} = 2/\{\sqrt{3}(L + D)^2 L\}$, which is continuous with the above small-axial-ratio ϱ_{cpd1} at $(D + L)/L \approx 2.38$. (Note also that $\nu\varrho_{cpd2}$ reduces to the disk value $\pi/\sqrt{12}$ in the limit $D \to \infty$.) Our result for ϱ_{cp} for torocylinders differs from that obtained by Taylor[24] and, as discussed below, gives rise to a somewhat different set of cell model predictions for phase behavior.

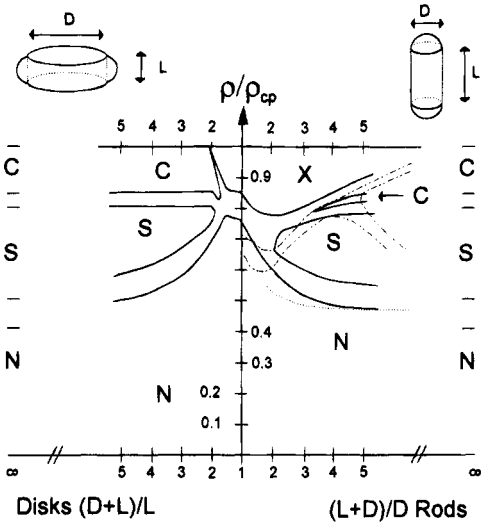

Figure 2. Phase diagram for hard rods and disks. The solid-line parts are the results obtained from our cell model, described in section II. The dotted- and dashed-line parts represent the simulation results of Stroobants et al.;[9] the dotted line represents the (second-order) N/S transition, and the dashed lines represent the (first-order) S/X, S/C, and C/X transitions.

We are now in a position to determine the phase coexistences by searching for common tangent constructions involving the free energies of the successively more positionally ordered states N, S, C, and X. In this way, we obtain the phase diagrams for rod and disk fluids. Taylor, Hentschke, and Herzfeld[28] and Taylor[24] have done this for aligned spherocylinders and for oblate spherocylindrical (= torocylindrical) disks, respectively. We have carried out a calculation similar to theirs except for two differences. First, we used the y expansion—vs scaled-particle theory—for describing the fluid entropies. This agrees with SPT for the one- and two-dimensional fluids but yields a slightly different phase boundary for the nematic, which involves 3-D entropy of packing effects. Second, we use an alternative expression for the disk close-packing density. The phase diagram found by Taylor et al.,[24,28] and the similar diagram which we have found, agree in a qualitative manner with the simulations of Stroobants et al.[9] Our results are presented in Figure 2, together with the rod coexistences obtained from the data of Stroobants et al. Note that we necessarily find a first-order N/S transition since we write separate free energies for each of these phases and f_S does not reduce to f_N as smectic order disappears. We could improve upon this situation, but this is unnecessary for our primary objective of predicting and understanding the *sequence* of the phase changes. The rod side of our phase diagram is essentially the same as that of Taylor et al.[28,24]—we find the same pairs of coexistence curves for the S/X, X/C, and C/S transitions, and only slight differences for S/N—while the disk side resembles Taylor's phase diagram for torocylinders,[24] except for differences in the parts involving the

crystalline phase (arising from different descriptions of close packing referred to above).

III. Monte Carlo Simulation Studies

Monte Carlo simulations of hard torocylinders are of interest for a number of reasons. The primary aim of such work is the extension of the hard particle phase diagram[9] to include disklike particles as well as rodlike ones and the testing of analytic theories which predict a disk phase diagram; see Figure 2. Because of its strongly curved edge, the torocylinder is a more realistic model of a disk-shaped particle than is either the right circular cylinder or (in the limit of large D/L) the cut sphere (see below).

All of the simulations described herein were isobaric Monte Carlo simulations[29] of systems of torocylinders of axial ratio $D/L = 5$. The isobaric (or constant-NPT) technique was used because it allows not just for volume fluctuations but also changes in the *shape* of the sample, thereby possibly allowing changes in phase to occur more easily. The torocylinders were perfectly aligned parallel to their cylindrical axes. As a control on our results, we also performed simulations of *spherocylinders* with 5:1 axial ratios—a system whose behavior is fairly well understood.[9,21b] All the disk simulations (with exceptions mentioned below) were carried out at a pressure $Pv/kT = 10$, where v is the particle volume (see ref 30). This pressure was chosen because we believed that it is not far above the smectic phase for $L/D = 5$ rods. (The density information we used to draw this conclusion is in ref 21b.) All simulations were of 1080 particles, a system size important in the previous literature.[21b] The initial states represented either perfectly ordered AAA solid structures (that is, solids consisting of stacked layers, each of which is hexagonally ordered, and with particles in one layer directly above those in the layer below; see ref 21b) or perfectly layered smectics (that is, stacks of planar layers, with particles in each layer randomly distributed in a nonoverlapping way). The simulation box was a rectangular parallelepiped, with the three box edges moved, one at a time, after one complete set of particle position moves. (Each sweep consisted of an attempt to move all particles. For a large sample such as we used, the overall results of this procedure should not differ significantly from those of other MC techniques in which one particle can be moved repeatedly. Moving all particles each time may separate local accumulations of particles more quickly than those techniques can.) Acceptance ratios for both particle moves and box edge moves were maintained between 0.2 and 0.6. For box edges, this ratio was recalculated every 20 steps.

Each sample was either 12 layers high in the alignment direction or three layers high. These heights were meant to allow us to control the (unphysical) diffusion of columns of particles in the direction of alignment. This diffusion arises from the overall motion of entire columns of particles in the directions of their column axes; it was described by Veerman and Frenkel,[21b] who suggested that effects like this may play roles in the artificial stabilization of columnar phases of rods. One can understand the origin of this diffusion in the following manner. When there are very few particles in a single column MC moves of the particle positions tend to push the entire column to and fro along its axis. These motions result in an overall drift of the column away from its initial position. Veerman and Frenkel[21b] found that a columnar phase of rods can appear in small samples but fails to appear in a similar sample containing a much larger number of rods, specifically having more layers. The columnar phases of the small samples consisted of crystallike columns of particles which were out of registry with each other and therefore did not exhibit overall layering. This finding suggests that the small-sample columnars really were more like crystals in which the columns had moved diffusively relative to one another.[21b] On the basis of these results, we conjectured that the presence of as many as 12 layers would effectively suppress column diffusion, while as few as three would not. In our 12-layer samples, each layer contained 90 particles, distributed randomly for smectic initial states and arranged in a 9 × 10 hexagonal lattice for AAA initial states (9 parallel rows of particles, 10 particles per row). In the 3-layer samples, the layers had 360 particles each, in an 18 × 20 hexagonal lattice if the sample was AAA.

TABLE 1: Parameters of the Rod and Disk Simulations

series name	initial state	particle	initial ϱ/ϱ_{cp}	layer spacing/L	no. of steps
A	3-layer AAA	rod	0.86	1.22	9 700
B	3-layer AAA	disk	0.86	1.05	5 000
1	12-layer AAA	rod	0.86	1.22	8 900
2	12-layer S	rod	0.40	1.5	78 500
3	12-layer AAA	disk	0.86	1.02	58 700
4	12-layer S	disk	0.40	1.3	146 800

When layers in samples like these are too small, then a layer diffusion effect, similar to the column diffusion effect but resulting in motions of layers, becomes possible.[21b] We do not think that this effect played a major role in our study, because we used samples in which the number of particles across a layer was close to or greater than the number of particles in a column. But even if layer diffusion were significant, it would tend to destabilize the columnar phase; hence, an observed columnar phase could not be an artifact of layer diffusion.

Six series of simulations were carried out; their parameters are described in Table 1. (In this description, a "step" is a full set of attempts to move the particle positions and the box edges, and a "series" is a sequence of consecutive steps, consisting of one or more actual runs of the simulation program.)

The density of $0.4\varrho_{cp}$ was chosen because it appeared to be slightly below the smectic phase for spherocylinders. This judgment was based on data in refs 9 and 21b. We also thought the low density of $0.4\varrho_{cp}$ would allow particles room to rearrange quickly. Based on our analytic calculations, the density of $0.86\varrho_{cp}$ was believed to be slightly above the columnar phase. This belief also is consistent with data in ref 21b.

Data from series A and B were used to check the importance of stack diffusion effects in these simulations. Comparison of the results of these series with the results of the other four series confirmed that diffusion of stacks is appreciable for the 3-layer samples, but not for the 12-layer samples. Accordingly, only series 1−4 were used to study rod/disk asymmetry. Series 1 and 2 for rods, and 3 and 4 for disks, had the same aim: to bring a fluid of particles of a given particle shape (rod or disk) to equilibrium starting with a smectic and, separately, from a crystal. Agreement of the "final" phases obtained from a smectic and a crystalline initial state would suggest that the common phase obtained is the "correct" (equilibrium) one.

We did not use a columnar initial state because of the possibility that such a state might give rise to a columnar state which is only kinetically stable and not in equilibrium. Such a state might be difficult to distinguish from an equilibrium columnar state. With smectic and solid initial states, a phase transition to a columnar state would provide evidence that the columnar is at least closer to equilibrium than was the initial state.

Identification of phases was accomplished in part by visual inspection of plots of the centroids of the particles and by calculation of pair correlation functions. The plots used included 2-D projections of the entire box along various axes and similar

TABLE 2: Results of the Rod and Disk Simulations

series name	final state	final ϱ/ϱ_{cp}
1	defective X	0.816
2	defective X	0.768
3	C	0.820
4	C	>0.775 (see text)

projections of slices of the box made by planes normal to the coordinate axes. The following pair correlation functions[31] also were calculated: (1) the total *parallel* pair correlation function, a normalized histogram of two-particle separations parallel to the z axis (that is, of Δz between particles); (2) the total *normal* pair correlation function, a normalized histogram of two-particle separations in the xy coordinates (that is, of $[(\Delta x)^2 + (\Delta y)^2]^{1/2}$); (3) the *intra*column parallel pair correlation function, a histogram of Δz for particle pairs which lie in the same column (a column was defined as a cylinder of diameter D for rods, or D or $D + L$ for disks); (4) the *inter*column pair correlation function, calculated like the intracolumn function except that the Δz of a pair is included if the two particles do *not* lie in the same column.

The intracolumn pair correlation functions were particularly useful for discriminating between the true columnar phases and AAA solids with stack diffusion parallel to the alignment direction. These functions were compared qualitatively with known 1-D pair correlation functions for hard particle fluids[32] and 1-D crystals.

The following system behaviors were taken as evidence of equilibrium: leveling-off of volume (with small fluctuations but no overall upward or downward trend), stabilization of the structure of the phase as indicated by unchanging pair correlation functions (with only small fluctuations), and persistence of observable structure in the centroid plots.

The preliminary series A and B confirmed the suspicion that "stack diffusion" would occur in samples three particles high. Interestingly, the disk columns also showed some signs of melting within the columns. Since these series were meant to check on the presence of column diffusion, they were not examined for equilibrium.

The final states for series 1−4 are described in Table 2.

Series 1 resulted in what appeared to be a solid. The structure of this crystal consisted of 12 distinct hexagonal layers, but in some cases adjacent layers were stacked in an irregular way (that is, neither "AA" nor "AB" type stacking). It was concluded that the phase was a crystal with defects. In series 2, the final state also appeared to be a defective solid. Its volume agreed with that of the final state of series 1 within 6%. In series 3 (disks from X), the final state appeared to be a columnar phase.[33] Both the hexagonal order in the transverse direction and the absence of layering were clearcut, as is apparent from the configuration snapshot in Figures 3 and 4 and from the pair correlation functions in Figures 5 and 6. The intracolumn pair correlation function was similar to that of a 1-D liquid, with successive peaks becoming wider and lower rather than remaining sharp and similar in height (see ref 32).

Series 4 had a complicated and interesting outcome. After about 60 000 steps the order and volume appeared to stop changing. At 94 300 steps, the volume still was fluctuating around 43 300L^3 (from an initial value of 84 000L^3). The order appeared to involve some layering and some hexagonal order; the order within the columns was reminiscent of a 1-D fluid. However, since the hexagonal order was rather diffuse and there still was appreciable layering, we conjectured that the sample was not at equilibrium but was in a local free energy minimum. To test this possibility, we altered the sample in various ways

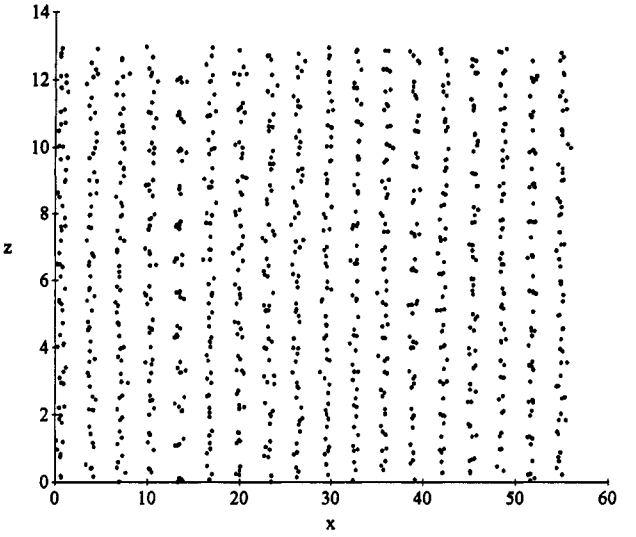

Figure 3. Projection in the xz plane (a plane parallel to the alignment axis) of the centers of mass in the final configuration from series 3. (Distance scales are in units of the particle height L.)

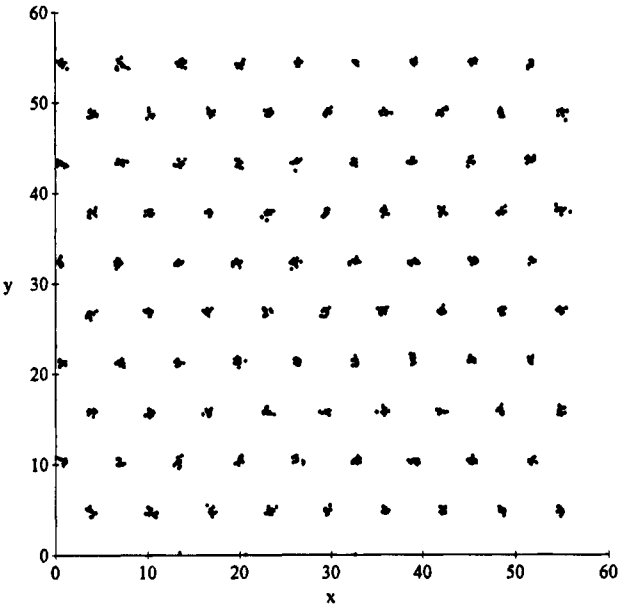

Figure 4. Projection in the xy plane (a plane normal to the alignment axis) of the final configuration (centers of mass) from series 3. (Distance scales are in units of the particle height L.)

to try to "coax" it to equilibrium. A dilation of 25% in the z direction, applied after 94 300 steps, resulted in a striking loss of layering and some enhancement of hexagonal order. The sample was observed for 42 500 steps, and this order persisted. The parallel pair correlation functions before the dilation and after the loss of layering are shown in Figures 7 and 8, respectively. Two further 5% dilations (after steps 136 800 and 144 300) resulted in some further loss of layering. These dilations resulted in little change in volume (i.e., the initial volume increases relaxed almost completely). Recall that absence of layering, with hexagonal order transverse to the alignment direction, is the signature of a columnar phase. (The transverse hexagonal order was documented for series 4 by checking for sharp peaks in the *radial* pair correlation function; we found results qualitatively similar to those in Figure 6.)

We also tried runs at elevated pressure to bring the sample to equilibrium. Starting with the configuration from series 4 obtained after 136 800 steps, we applied a pressure Pv/kT = 15 (vs the original value of 10) for 36 000 steps. This resulted

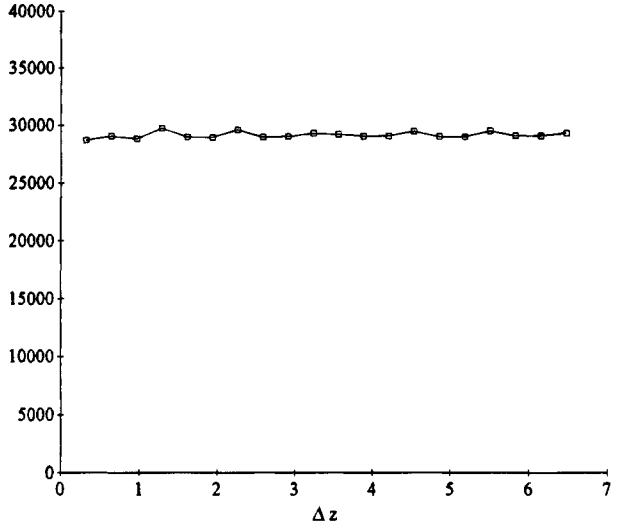

Figure 5. Parallel pair correlation function from the last 5000 steps of series 3. (The horizontal scale is in units of the particle height L; the vertical scale is in arbitrary units.)

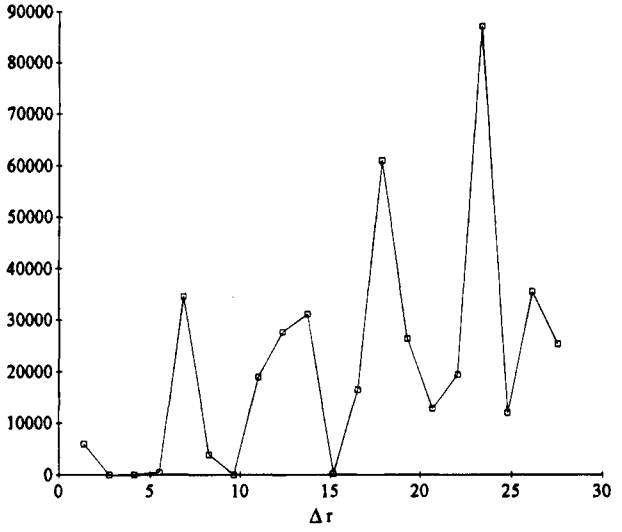

Figure 6. Radial pair correlation function from the last 5000 steps of series 3. (The horizontal scale is in units of the particle height L; the vertical scale is in arbitrary units.)

in a columnar phase of volume 41 400L^3, which persisted for 13 000 steps at the same pressure. Another series with Pv/kT = 20, beginning from the configuration at 33 000 steps in the Pv/kT = 15 series, resulted in a columnar with a volume of 41 000L^3. At Pv/kT = 10, the configuration expanded to a columnar of volume 41 700L^3.

To further test the stability of the columnar phase of disks, we dilated the final configuration of series 3 in the z direction and compressed it at Pv/kT = 10. A 10% dilation, followed by a 3000-step run, resulted in a volumne of 43 000L^3, still declining. The phase remained columnar. Two similar runs beginning with smaller dilations also failed to produce a phase change.

Finally, we ran an independent simulation beginning from an ABC, or face-centered cubic, solid of density 0.86ϱ_{cp}. Since a fcc solid does not have the simple hexagonal order of an AAA phase, it should be more difficult to melt to a columnar. Hence, if the ABC solid does melt to a columnar at the same pressure at which the AAA seems to, this would suggest that the columnar is the correct equilibrium phase at that pressure. After 2500 steps, the volume expanded from 39 200L^3 to 39 700L^3. Although the sample had not yet reached equilibrium, the

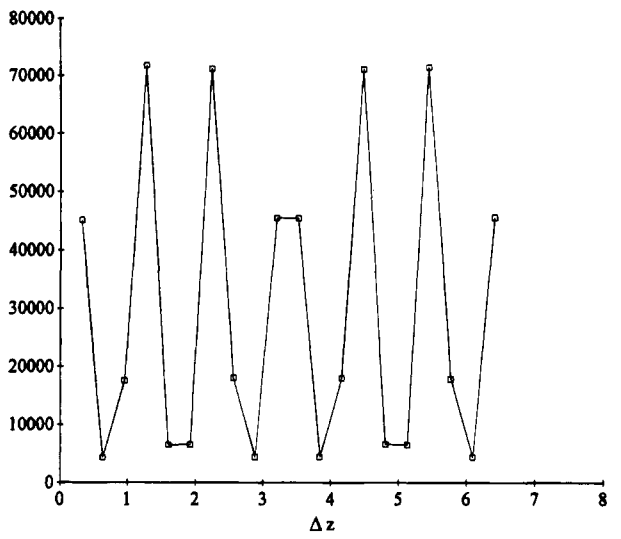

Figure 7. Parallel pair correlation function from the last 5000 steps of series 4, before the first dilation. (The horizontal scale is in units of the particle height, L; the vertical scale is in arbitrary units.)

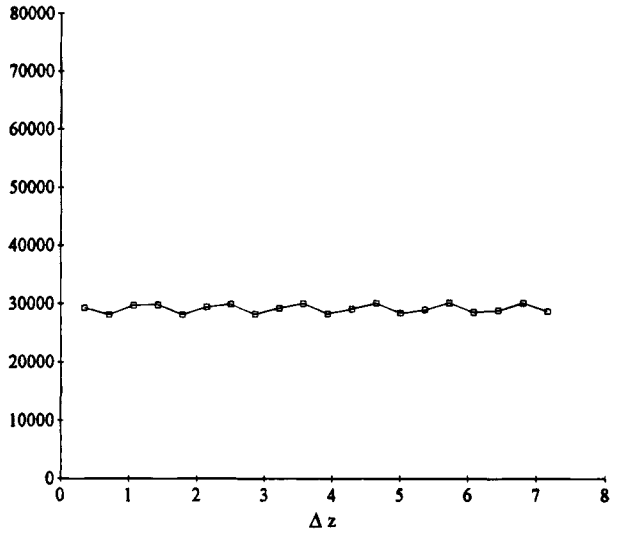

Figure 8. Parallel pair correlation function from the last 5000 steps of the run between the first and second volume dilations, that is, after relaxation of layering. (The horizontal scale is in units of the particle height L; the vertical scale is in arbitrary units.)

relaxation of layering was conspicuous. This outcome is consistent with our hypothesis that the columnar is the stable phase.

IV. Concluding Remarks

In the above discussion we have presented the similar and contrasting results for rods vs disks obtained from analytical theories of aligned hard particles on the one hand and from hard particle Monte Carlo simulations on the other. It appears that the physically pleasing cell models are not sufficiently accurate to treat correctly the delicate packing and free energy differences between competing modes of positional ordering in these systems. In particular, the analytical theories predict a highly symmetrical phase diagram with respect to aligned prolate and oblate particles, whereas the preliminary Monte Carlo simulations presented here suggest that the columnar phase is much more likely for disks than for rods.

Related attempts to illuminate the phase behavior of hard disks have been reported for "cut spheres" (spheres bounded by two parallel planes equidistant from the center) by Veerman

and Frenkel[22] and by Azzouz et al.[23] In the former case, the cut sphere disks with axial ratio 10:1 are allowed all orientations, and the sequence N → C → X is observed. Azzouz et al., on the other hand, consider the case of perfect alignment and find a N → S transition for this same axial ratio, with no evidence of a columnar phase. Finally, Taylor and Herzfeld[34] have investigated the phase behavior of imperfectly aligned *spheroplatelets* (the volume swept out by a sphere having radius a with its center confined to a $b \times c$ rectangle) and found an asymmetry in rod vs disk behavior which, for a 5 to 1 rod (disk), shows a relatively large (small) density range of smectic phase and a small (large) range of columnar states. Given the recently established marginality of the columnar phase,[21b] the strong dependence on precise shapes ("end effects") (see refs 9 and 35), and the several possibilities for crystalline orderings of aligned sphero-/torocylinders, it is clear that much work remains to be done before a simple understanding emerges for the relative stabilities of layered and hexagonal states of colloidal rods and disks.

Acknowledgment. We are pleased to acknowledge many helpful discussions with Prof. Zhen-Gang Wang and Dr. Carey Bagdassarian. This research has benefited from financial support from the U.S. National Science Foundation (Grant CHE 92-01166) and the Yeshaya Horowitz Association. The Fritz Haber Center, of which A.B.-S. is a member, is supported by the Minerva Gesellschaft fur die Forschung, Munich, Germany. Some parts of this work benefited from the assistance of the UCLA Office of Academic Computing. We thank Dr. Mark P. Taylor for permission to publish Figure 2, which in part resembles Figure 1 in ref 28 and Figures 4.2 and 4.5 in ref 24. We thank the American Physical Society for permission to publish Figure 2, which in part resembles Figure 1 in ref 28, and the American Physical Society and Dr. H. N. W. Lekkerkerker for permission to publish the redrawn version (part of our Figure 2) of Figure 9 in ref 9. Finally, we thank University Microfilms International for assistance with MFS's doctoral dissertation (ref 36), in which the work described in this paper (and, in particular, other versions of the figures) will again appear.

Appendix. Close-Packing Density of Torocylinders

Throughout this paper we have used a particular expression for the close-packing volume of torocylinders. In this Appendix we present our argument for this expression. Although we believe the expression to be physically plausible, we have not found a rigorous proof. The question of the correct close-packing density remains open; indeed, it is very difficult to prove any such expression rigorously. It is important to note that Taylor[24] has used an expression for the unit cell volume of torocylinders which differs from ours.

In the limit $D = 0$, torocylinders reduce to hard spheres. For $D \ll L$, we expect the close packing for torocylinders to be similar to that of spheres, with each particle "nestling" in the space defined by three particles in the next layer. As D grows large compared to L, the disks eventually become too wide to nest in this way. The diameter of the disk increases linearly with D, but the size of the space in which the disk can nest depends upon the thickness of the toroidal rims of the three disks below it (that is, L). Hence as D increases, the disk eventually "outgrows" its "nest".

When the torocylinders become too large, the cylindrical core of each particle overhangs the edges of the cylindrical cores of the particles in the layer below it (see Figure 9). In this case, the upper disk cannot nest among the disks below but sits with its flat bottom on the flat tops of the lower disks. This overlap occurs when $s < D$, where s is the distance shown in Figure 9. Hence, for $D > D_{crit} = L/(\sqrt{3} - 1)$, disks cannot "nest" as spheres do, unless the particles in the layer below spread apart to accommodate the disks on top. One can think of this disruption of the spherelike packing as a frustration effect.

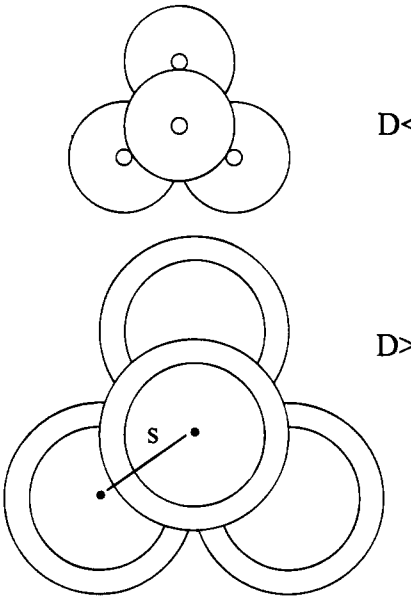

Figure 9. Packing of torocylinders in the limits of narrow disks ($D \ll L$) and of wide disks ($D \gg L$).

Now we make a key assumption: that the close-packed configuration for torocylinders with $D < D_{crit}$ consists of a stack of hexagonal layers of torocylinders, with the particles in each layer sitting over the holes in the layer below. (Let us call this an "SHL" or staggered hexagonal-layered configuration.) For $D = 0$ and for $D = D_{crit}$, the close-packed configurations are SHL (spherelike and cylinderlike, respectively). The following argument (which makes certain tacit assumptions) suggests that the close-packed configuration for any D is a SHL configuration.

Beginning with the $D = 0$ configuration and allowing the cylindrical cores to grow, we see that we can construct a SHL configuration for any D (though adjacent particles may not always touch). Consider the least upper bound $\varrho_{shl}(D)$ of densities of all SHL configurations and the true close-packed density $\varrho_{cp}(D)$ as functions of D. At $D = 0$, $\varrho_{shl}(D)$ and $\varrho_{cp}(D)$ agree. Take the close-packed configuration at $D = 0$ and let D increase. Suppose that one reaches values of D where $\varrho_{cp}(D) > \varrho_{shl}(D)$. Take the greatest lower bound D_0 of these values of D. For D just below D_0, the two densities are equal; at or just above D_0, $\varrho_{shl}(D)$ is lower. There are two possibilities:

1. The difference $\varrho_{cp}(D) - \varrho_{shl}(D)$ might have a finite jump at D_0. In that case, we can take the close-packed configuration C_1 at $D = D_0 + \delta$ (δ small) and let the disks shrink by an infinitesimal amount $\Delta D = -2\delta$ while preserving the original geometry. (We may have to change the interlayer or intralayer spacing infinitesimally to do this.) This results in a configuration with $D = D_0 - \delta$, but with density differing infinitesimally from that of C_1, hence higher than that of the SHL configuration at $D = D_0 - \delta$. This contradicts the assumption that the close-packed configuration is SHL for $D < D_0$.

2. The difference $\varrho_{cp}(D) - \varrho_{shl}(D)$ might be continuous at D_0. Then there is a non-SHL close-packed configuration whose density equals $\varrho_{shl}(D)$ for some D, and then exceeds it and rises continuously with increasing D. This is physically implausible for the following reason. If we start with the $D = 0$ crystal (nested spheres) and allow the cylindrical cores to grow larger,

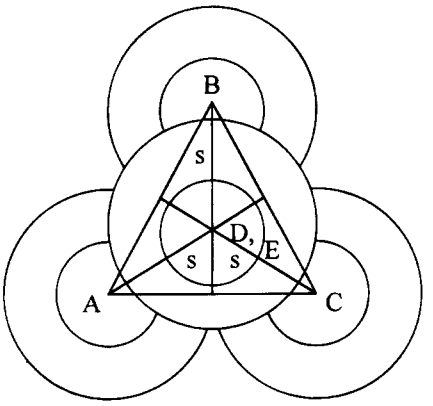

Figure 10. Part of a typical staggered hexagonal-layered (SHL) configuration of torocylinders.

the expansion of the cores of the disks will expand each layer of disks and also will tend to raise the nested disks out of their holes. The hexagonal arrangement of particles in a layer is a tight packing; the space in the layers is used efficiently, and particles from the next layer up nestle rather deeply in the holes in a layer, compared to (for example) a square arrangement. Hence as D increases, a particle in the next layer up will be forced out of its "nest" less in the SHL configuration than in other configurations. This suggests that the volume of the SHL configuration will rise more slowly with increasing D than that of other candidates for the close-packed configuration, so its density—higher at $D = 0$—will remain higher for all D. (We have ignored the possibility that increasing D leads to spreading within layers instead of ejection of the nestled particle from its nest. But that would not affect the physical argument, since this effect will be less pronounced if layers are tightly packed.)

Once we make the physically plausible assumption that the close-packed configuration is SHL, we can derive the density as follows.

Figure 10 shows a representative piece of a SHL configuration of torocylinders, viewed along the axis of particle alignment (which is normal to the page). Points A, B, and C lie in one layer; they are centers of mass of particles (also called A, B, and C) in one layer of the crystal. Point D is the center of mass of a particle in the next layer, which nests in the space between particles A, B, and C. Point E is the point in the plane of A, B, and C which lies directly below point D. In the close-packed configuration, particle D will touch particles A, B, and C, since moving D out of contact will increase the volume of the crystal without improving the packing.

Let s = AE = CE = BE. The area of triangle ABC is $((3\sqrt{3})/4)s^2$. Using the fact that the half-toroidal rims of particles in neighboring layers touch, it follows that the height difference (h) between centers is $h = [L^2 - (s - D)^2]^{1/2}$. This yields the following 3-D particle density: $\varrho = 1/\{[(3\sqrt{3})/2]\, s^2\, [L^2 - (s - D)^2]^{1/2}\}$. To find the close-packing density, we maximize ϱ with respect to s or, equivalently, minimize $f(s) = s^4[L^2 - (s - D)^2]$.

We need to minimize $f(s)$ only for D within the "nestling" range $0 < D < D_{crit}$ and only within the interval $[s_{min}, s_{max}]$, where $s_{min} = (L + D)/\sqrt{3}$ and $s_{max} = (\sqrt{3}/2)L + D$. For $s = s_{min}$, the particles in each layer become close-packed within the layer; hence, s cannot be smaller. For $s > s_{max}$, the layers on either side of a given layer come into contact with one another, so s cannot increase further.

Differentiation of $f(s)$ yields a quadratic with two real roots. The minus root appears to be less than s_{min} for all values of D between 0 and D_{crit} and hence is unphysical. Hence, the plus root, s_+, is the only possible extremum of f except for s_{min} or s_{max}. That is, f either is concave downward with s_+ as a global minimum or is concave upward with either s_{min} or s_{max} as a global minimum. For all relevant values of D, df/ds is positive at $s = s_{min}$. Hence, either s_{min} or s_{max} is the global minimum. Direct algebraic comparison of $f(s_{min})$ and $f(s_{max})$ reveals that $f(s_{min}) < f(s_{max})$. Thus, s_{min} is the minimum of f and the maximum of ϱ. Substituting $s = s_{min}$ in the above expression for $\varrho(s)$ yields our expression for ϱ_{cp} for disks.

References and Notes

(1) Onsager, L. *Ann. N.Y. Acad. Sci.* **1949**, *51*, 627.
(2) Tjipto-Margo, B.; Evans, G. T. *J. Chem. Phys.* **1990**, *93*, 4254.
(3) Gelbart, W. M. *J. Phys. Chem.* **1982**, *86*, 4298.
(4) See, for example: Vieillard-Baron, J. *Mol. Phys.* **1974**, *28*, 809. Kushick, J.; Berne, B. J. *J. Chem. Phys.* **1976**, *64*, 1362.
(5) Frenkel, D.; Eppenga, R. *Phys. Rev. Lett.* **1982**, *49*, 1089. Frenkel, D.; Mulder, B. M.; McTague, J. P. *Phys. Rev. Lett.* **1984**, *52*, 287. Frenkel, D.; Mulder, B. M.; McTague, J. P. *Mol. Cryst. Liq. Cryst.* **1985**, *123*, 119.
(6) Fraden, S.; Maret, G.; Caspar, D. L. D.; Meyer, R. B. *Phys. Rev. Lett.* **1989**, *63*, 2068.
(7) Oldenbourg, R.; Wen, X.; Meyer, R. B.; Caspar, D. L. D. *Phys. Rev. Lett.* **1988**, *61*, 1851.
(8) See: Hoover, W. G.; Ree, F. H. *J. Chem. Phys.* **1968**, *49*, 3609.
(9) Stroobants, A.; Lekkerkerker, H. N. W.; Frenkel, D. *Phys. Rev. A.* **1987**, *36*, 2929.
(10) Wen, X.; Meyer, R. B.; Caspar, D. L. D. *Phys. Rev. Lett.* **1989**, *63*, 2760.
(11) Taylor, M. P.; Hentschke, R.; Herzfeld, J. *Phys. Rev. Lett.* **1989**, *62*, 800. Hentschke, R.; Taylor, M. P.; Herzfeld, J. *Phys. Rev. A* **1989**, *40*, 1678. See also Taylor, M. P.; Herzfeld, J. *Langmuir* **1990**, *6*, 911.
(12) Somoza, A. M.; Tarazona, P. *Phys. Rev. Lett.* **1988**, *61*, 2566.
(13) Poniewierski, A.; Hołyst, R. *Phys. Rev. Lett.* **1988**, *61*, 2461.
(14) Wen, X.; Meyer, R. B. *Phys. Rev. Lett.* **1987**, *59*, 1325.
(15) Mulder, B. *Phys. Rev. A* **1987**, *35*, 3095.
(16) Taylor, M. P.; Herzfeld, J. *Phys. Rev. A* **1991**, *43*, 1892.
(17) Stroobants, A. *Phys. Rev. Lett.* **1992**, *69*, 2388.
(18) Taylor, M. P.; Herzfeld, J. *Langmuir* **1990**, *6*, 911.
(19) Boden, N. In *Micelles, Membranes, Microemulsions and Monolayers*; Gelbart, W. M.; Ben-Shaul, A.; Roux, D., Eds.; Springer-Verlag: New York: 1994.
(20) Frenkel, D.; Lekkerkerker, H. N. W.; Stroobants, A. *Nature* **1988**, *332*, 822.
(21) (a) Veerman, J. A. C.; Frenkel, D. *Phys. Rev. A* **1990**, *41*, 3237; (b) **1991**, *43*, 4334.
(22) Veerman, J. A. C.; Frenkel, D. *Phys. Rev. A* **1992**, *45*, 5632.
(23) Azzouz, H.; Caillol, J. M.; Levesque, D.; Weis, J. J. *J. Chem. Phys.* **1992**, *96*, 4551.
(24) Taylor, M. P. *Statistical Mechanical Models of Liquid Crystalline Ordering in Reversibly Assembling Lyotropic Systems*; University Microfilms: Ann Arbor, 1991.
(25) Hentschke, R.; Taylor, M. P.; Herzfeld, J. *Phys. Rev. A* **1989**, *40*, 1678.
(26) For an introduction to scaled particle theory, see: Reiss, H. In *Statistical Mechanics and Statistical Methods in Theory and Application*; Landman, U.; Ed.; Plenum Press: New York, 1977.
(27) Barboy, B.; Gelbart, W. M. *J. Chem. Phys.* **1979**, *71*, 3053.
(28) Taylor, M. P.; Hentschke, R.; Herzfeld, J. *Phys. Rev. Lett.* **1989**, *62*, 800.
(29) See: Allen, M. P.; Tildesley, D. J. *Computer Simulation of Liquids*; Clarendon: Oxford, 1987.
(30) McMullen, W. E.; Ben-Shaul, A.; Gelbart, W. M. *J. Colloid Interface Sci.* **1984**, *98*, 523.
(31) On various pair correlation functions, see: Veerman, J. A. C.; Frenkel, D. *Phys. Rev. A* **1992**, *45*, 5632.
(32) See: Reiss, H.; Casberg, R. V. *J. Chem. Phys.* **1974**, *61*, 1107. Salsburg, Z. W.; Zwanzig R. W.; Kirkwood, J. G. *J. Chem. Phys.* **1953**, *21*, 1098.
(33) We should mention that at one point in the calculation one of the particles was moved manually by an amount $10^{-6}L$ in the z direction. This was done because two particles had happened to come extremely close—a situation which could slow or halt the simulation unnecessarily. A change this small should not affect the final results.
(34) Taylor, M. P.; Herzfeld, J. *Phys. Rev. A* **1991**, *44*, 3742.
(35) Frenkel, D. *Liq. Cryst.* **1989**, *5*, 929.
(36) Sharlow, M. F. *Liquid Crystalline Phases of Hard Rods and Disks*; University Microfilms: Ann Arbor, in press.

JP942322T